Simultaneous assessment of *in vitro* lipolysis and permeation in the mucus-PVPA model to predict oral absorption of a poorly water soluble drug in SNEDDSs

Margherita Falavigna[a], Sunniva Brurok[a], Mette Klitgaard[b], Gøril Eide Flaten[a*]

[a] Drug Transport and Delivery Research Group, Department of Pharmacy, UiT The Arctic University of Norway, Universitetsveien 57, 9037 Tromsø, Norway. margherita.falavigna@uit.no; sunnivabrurok@gmail.com; goril.flaten@uit.no.

[b] Physiological Pharmaceutics, Department of Pharmacy, University of Copenhagen, Universitetsparken 2-4, 2100, Copenhagen, Denmark. mette.klitgaard@sund.ku.dk.

*Corresponding author

Abstract

The prediction of the *in vivo* performance of self-nanoemulsifying drug delivery systems (SNEDDSs) is currently gaining increasing attention. Therefore, the need for reliable *in vitro* models able to assess the drug solubilization capacity of such formulations upon *in vitro* lipolysis, as well as to concomitantly evaluate *in vitro* drug permeation, has become ever so evident. In the current study, the high-throughput *in vitro* intestinal lipolysis model was combined with the mucus-PVPA *in vitro* permeation model to study the solubilization capacity of SNEDDSs for the poorly water-soluble drug fenofibrate and to study the consequent drug permeation. Moreover, drug solubilization and permeation were evaluated both in the presence and absence of lipolysis. The results obtained demonstrated that the presence of *in vitro* lipolysis significantly impacted the solubilization and permeation profiles of fenofibrate compared to its absence. The results were in accordance with already published *in vivo* data regarding the same fenofibrate-loaded SNEDDSs. Additionally, the correlation between the *in vitro* permeation data and *in vivo* plasma concentration in rats was found to be excellent both in the presence and absence of lipolysis ($R^2 > 0.98$), highlighting the ability of the developed combined *in vitro* model to predict *in vivo* drug absorption.

Keywords: *In vivo-in vitro* correlation (IVIVC); *in vitro* permeation; *in vitro* lipolysis; lipid-based formulation; oral drug delivery; poorly water-soluble drugs.

1. Introduction

The complexity of the physiological processes and characteristics of the gastrointestinal (GI) tract have shown to greatly affect the therapeutic outcome of oral drug-delivery systems (Lin et al., 2017). For instance, drug absorption can be largely influenced by the pH condition of the specific GI compartment, the presence and activity of metabolic enzymes and by the presence and composition of the food components possibly present along the GI tract (Vertzoni et al., 2019). These factors can have different effects on drug absorption according to the specific administered drug and its physicochemical characteristics. In particular, as up to 70 % of new drug entities have been shown to be poorly water-soluble, increasing focus has been put on developing formulations able to overcome the low bioavailability connected to this type of drugs, and to understand the physiological processes affecting the performance of such formulations (Berben et al., 2018). In particular, lipid-based formulations such as self-nanoemulsifying drug delivery systems (SNEDDSs) have shown to improve the bioavailability of poorly water-soluble drugs (PWSD) thanks to enhancement of solubilization and permeation, lymphatic transport and stimulation of supersaturation (Gao and Morozowich 2006; Porter et al., 2007; Siqueira et al., 2017; Trevaskis et al., 2008). The dispersion of these formulations into the gastric and intestinal fluids and the digestion processes initiated by digestive enzymes are two of the ~~main~~ key factors affecting the performance of SNEDDSs and the related drug absorption (Feeney et al., 2016). Even though several SNEDDSs have already reached the market, their optimization is still regarded as challenging due to the complex array of the processes (*i.e.* equilibrium between SNEDDSs digestion, drug supersaturation, precipitation and absorption) that can affect their performance (Savla et al., 2017). Due to the challenges related to predicting the behavior of these lipid-based formulations, the need for *in vitro* models able to evaluate the *in vivo* performance of SNEDDSs has become ever so evident. Consequently, several research efforts initially focused on producing *in vitro* models able to either study

the effect of digestive enzymes on the *in vitro* drug solubilization capacity of SNEDDSs (*i.e.* the *in vitro* intestinal lipolysis model (Zangenberg et al., 2001)), or on evaluating the *in vitro* permeation of PWSDs with the use of permeation barriers (*i.e.* the Caco-2 model (Artursson et al., 2001); the PAMPA model (Kansy et al., 1998); the PVPA model (Flaten et al., 2006); the Permeapad™ (di Cagno et al., 2015); and the AMI system (Berben et al., 2018)). However, the separate evaluation of *in vitro* lipolysis and *in vitro* drug permeation did not lead to a complete overview of the physiological processes affecting oral drug absorption. In fact, it has been shown that the evaluation of drug solubilization upon *in vitro* lipolysis of lipid-based formulations in the absence of an absorptive sink overestimates drug supersaturation and precipitation and underestimates drug absorption, while the addition of a permeation step leads to a more representative prediction of oral drug absorption *in vivo* (Bevernage et al., 2012; Stillhart et al., 2014). As a result of this, these two processes have been pooled together to produce combined *in vitro* lipolysis-permeation models (Alskär et al., 2019; Berthelsen et al., 2019; Bibi et al., 2017; Hedge and Bergström 2020; Ille et a., 2020; Keemink et al., 2019; Keemink and Bergström, 2018; O'Dwyer et al., 2020). These combined models proved to predict the *in vivo* drug absorption from SNEDDSs to a higher extent compared to *in vitro* lipolysis or *in vitro* permeation alone. However, all of the mentioned models except one (Keemink and Bergström, 2018) lack the presence of a mucus layer on top of the permeation barriers, thus not being able to closely mimic the physiology of the GI mucosa (Falavigna et al., 2020a; Lechanteur et al., 2018). Notably, it has been shown that the presence of the mucus layer can stabilize supersaturation of PWSDs after *in vitro* lipolysis of lipid-based formulations, and it has been proposed that this could be one of the intrinsic mechanisms of action of these formulations (Yeap et al., 2013; Yeap et al., 2019). Further, several studies have pointed at the influence that mucus has on the diffusion and permeation of PWSDs, thus further emphasizing the importance of taking this additional barrier into account (Falavigna et al., 2020b; Miyazaki et al., 2019). To account for the need of mucus in a combined *in vitro* lipolysis-permeation model, a biosimilar mucus layer was added on top of the PVPA (Phospholipid Vesicle-based Permeation Assay) barriers (*i.e.* mucus-PVPA barriers) (Falavigna et al., 2020a). The mucus-PVPA barriers were used in combination with the *in vitro* intestinal lipolysis model equipped with a pH-stat-titration apparatus (Falavigna et al., 2020a), and it was found that the combined *in vitro* lipolysis-permeation model was able to predict the *in vivo* oral

absorption of fenofibrate from SNEDDSs for which *in vivo* data was available in the literature (Falavigna et al., 2020a; Michaelsen et al., 2019). However, while the above-mentioned combined models provided insightful information in the prediction of *in vivo* absorption data, ~~they all~~ for the most part they share the dependence from a pH-stat-titration apparatus to conduct the *in vitro* lipolysis step, thus limiting them to the availability of such laboratory equipment.

In light of the limitations connected to the already available combined *in vitro* models, the current study utilized the pH-stat-titration independent *in vitro* lipolysis model (*i.e.* the high-throughput (HTP) intestinal lipolysis model) developed by Mosgaard and colleagues (Mosgaard et al., 2015), in combination with the mucus-PVPA *in vitro* permeation model to study the performance of three fenofibrate-loaded SNEDDSs. ~~In the specific~~Specifically, the HTP *in vitro* intestinal lipolysis model has previously shown to predict drug distribution between aqueous, oil and pellet phase during lipolysis of SNEDDSs in the same manner as the *in vitro* intestinal lipolysis model, while not being tied to a pH-stat-titration apparatus (Mosgaard et al., 2015; Mosgaard et al., 2017). In fact, the high buffer capacity of the HTP intestinal medium is able to prevent the pH drop usually occurring after the release of free fatty acids from the digested SNEDDSs (Mosgaard et al., 2015), thus leading to a constant pH and eliminating the need for the pH-stat titrator. The mucus-PVPA barriers were chosen as the *in vitro* permeation model because of their ability to provide the combination of a biosimilar mucus layer with a permeation barrier, and as these barriers have previously proven to mimic the intestinal mucosa physiology (Falavigna et al., 2018; Falavigna et al., 2019). More specifically, the mucus-PVPA barriers allow the assessment of passive drug diffusion from their donor to the acceptor compartment similarly to other cell-free *in vitro* permeation tools used to assess intestinal drug permeation (*i.e.* PAMPA model (Kansy et al., 1998); Permeapad™ (di Cagno et al., 2015); AMI system (Berben et al., 2018)). The mentioned cell-free tools are not able to take into account the active and carrier-mediated transport occurring when a drug is being absorbed *in vivo*. However, even though an underestimation of active and carrier-mediated transport is a consequence of the mentioned tools, they provide a good estimation of *in vivo* passive drug diffusion, which is thought to be the predominant transport mechanism especially for lipophilic drugs (Dahlgren and Lennernäs, 2019).

The results obtained were compared to *in vivo* absorption data obtained by Michaelsen and colleagues (Michaelsen et al., 2019), where the same fenofibrate-loaded SNEDDSs were administered to rats, and for which no *in vivo-in vitro* correlation (IVIVC) was found when comparing the *in vivo* absorption data with *in vitro* lipolysis data. To evaluate if the model developed in the present study would predict the *in vivo* data collected by Michaelsen and colleagues (Michaelsen et al., 2019), the correlation between this *in vivo* data and the *in vitro* data obtained in the present study was evaluated.

2. Materials and methods

2.1. Materials

Acetonitrile CHROMANORM® (High-Performance Liquid Chromatography, HPLC, grade), ethanol NORMAPUR® 96%, v/v (HPLC grade), methanol CHROMANORM® (HPLC grade) were purchased from VWR (Radnor, PA, USA). Bile bovine, Bis-Tris, bovine serum albumin (BSA), 4-bromophenylboronic acid (BBBA), calcein, calcium chloride dihydrate ($CaCl_2 \cdot 2H_2O$), chloroform, cholesterol, dimethyl sulfoxide (DMSO), fenofibrate, hydrochloric acid (HCl), magnesium sulfate ($MgSO_4$), maleic acid, MES hydrate, mucin from porcine stomach type II, pancreatin from porcine pancreas, potassium phosphate monobasic, sodium chloride (NaCl), sodium hydroxide (NaOH), sodium phosphate dibasic dodecahydrate, soybean oil, Tween® 80, Trizma® base were products of Sigma-Aldrich (St. Louis, MO, USA). Ethanol 99.9% (v/v) was purchased from Arcus AS (Oslo, Norway). Kolliphor RH-40 was purchased from BASF (Ludwigshafen, Germany). Lipoid egg phospholipids E80 (80% phosphatidylcholine, PC) and Lipoid soybean lecithin S100 (>94% PC S100) were kindly gifted from Lipoid GmbH (Ludwigshafen, Germany), while Maisine CC was kindly donated from Gattefossé (St. Priest, France). Polyacrylic acid (Carbopol® 974 PNF, PAA) was obtained from Lubrizol (Brussels, Belgium). All chemicals employed were of analytical grade.

2.2. Methods

In this study, the mucus-PVPA barriers were used to assess the *in vitro* permeation of fenofibrate from three different SNEDDSs (*i.e.* super-SNEDDS solution$_{150}$, SNEDDS$_{75}$ and super-SNEDDS suspension$_{150}$) in the absence or presence of *in vitro* lipolysis utilizing the HTP *in vitro* intestinal lipolysis model. The results obtained from the *in vitro* lipolysis and permeation experiments were compared to *in vivo* plasma concentration of fenofibrate in rats after administration of the same SNEDDSs to assess the IVIVC between these sets of data.

2.2.1. Preparation of the mucus-PVPA barriers

2.2.1.1. Biosimilar mucus

Biosimilar mucus (BM) was prepared according to the method described by Boegh and colleagues (Boegh et al., 2014) and as described in Table 1. Specifically, PAA was dissolved in non-isotonic buffer (10 mM MES, 1.3 mM $CaCl_2$, 1.0 mM $MgSO_4$) and mucin was added and stirred until homogeneously dispersed. In parallel, a lipid mixture was prepared by mixing PC S100 lipids, cholesterol and Tween® 80 in isotonic buffer (10 mM MES, 1.3 mM $CaCl_2$, 1.0 mM $MgSO_4$, 137 mM NaCl). Finally, the lipid mixture and BSA were added to the PAA mixture, and stirred until homogeneity was reached. The pH of the final mixture (BM) was adjusted to 6.5.

Components	Ratio (w/v) %
PAA	0.90
Mucin	5.00
Cholesterol	0.36
PC S100	0.18
Tween® 80	0.16

BSA	3.10

153

154 **Table 1:** Composition of biosimilar mucus (BM).

155

156 *2.2.1.2. Mucus-PVPA barriers*

157 The PVPA barriers were prepared following the method previously described (Falavigna et al., 2018;
158 Falavigna et al., 2019). Briefly, liposomes with two different size distributions (0.4 and 0.8 µm) were
159 immobilized by series of centrifugation and freeze-thawing on top of membrane filters (nitrocellulose,
160 pore size 0.65 µm) fused on Transwell inserts (Corning Inc., New York, USA).

161 To produce the mucus-PVPA barriers, BM (50 µL) was deposited on top of the PVPA barriers 10
162 minutes prior to the start of the permeation experiment.

163

164 *2.2.2. Preparation of high-throughput intestinal medium*

165 The HTP intestinal medium was prepared according to the method described by Mosgaard and
166 colleagues (Mosgaard et al., 2015), as illustrated in Table 2. Briefly, the HTP intestinal medium was
167 prepared by weighing the components listed in Table 2 and dissolving them in MilliQ water. Finally,
168 the pH of the HTP intestinal medium was adjusted to 6.5. Calcein (5 mM) was added to the HTP
169 intestinal medium to determine its permeability across the mucus-PVPA barriers, and thus to assess their
170 integrity (see Section 2.2.4.2).

171

Components	Concentration (mM)
Bile bovine	2.96
PC S100	0.26
$CaCl_2 \cdot 2\ H_2O$	4.50

Bis-Tris	200

Table 2: Composition HTP intestinal medium.

2.2.3. Preparation of fenofibrate-loaded SNEDDSs

The fenofibrate-loaded SNEDDSs were prepared starting from a SNEDDS pre-concentrate according to the method described by Michaelsen and colleagues (Michaelsen et al., 2019). Briefly, the SNEDDS pre-concentrate was obtained by heating soybean oil, Maisine CC and Kolliphor RH-40 at 50 °C, and by mixing them in the following ratio: soybean oil-Maisine CC (1:1 w/w) 55% (w/w), Kolliphor RH-40 35% (w/w). Ethanol 99.9% (v/v) was added (10% (w/w)) once the mixture reached room temperature. The pre-concentrate was stirred until homogeneous at room temperature (23-25 °C).

Fenofibrate was added to the pre-concentrate to yield three different fenofibrate-loaded SNEDDSs, namely super-SNEDDS solution$_{150}$, SNEDDS$_{75}$ and super-SNEDDS suspension$_{150}$. SNEDDS$_{75}$ and super-SNEDDS suspension$_{150}$ were obtained by adding to the SNEDDS pre-concentrate an amount of fenofibrate corresponding to 75% and 150% of its equilibrium solubility, respectively (fenofibrate equilibrium solubility in the SNEDDS pre-concentrate: 88.5 mg/g (Thomas et al., 2014)). SNEDDS$_{75}$ and super-SNEDDS suspension$_{150}$ were left to stir at room temperature (23-25 °C) until homogeneity was reached. Fenofibrate was completely dissolved in the SNEDDS$_{75}$ (concentration lower than the equilibrium solubility), whereas for super-SNEDDS suspension$_{150}$ the drug was found both solubilized and in suspension (concentration higher than the equilibrium solubility). The super-SNEDDS solution$_{150}$ was obtained by dissolving an amount of fenofibrate corresponding to 150% of its equilibrium solubility to the SNEDDS pre-concentrate. To aid the complete solubilization of the drug in the pre-concentrate (*i.e.* avoid the formation of a suspension above the equilibrium solubility), the super-SNEDDS solution$_{150}$ was bath-sonicated for 30 minutes, heated at 60 °C for 3 hours and then let cool down at 37 °C overnight.

197 *2.2.4. In vitro lipolysis-permeation experiment*

198 This study focused on the development of a model where *in vitro* lipolysis and permeation could occur
199 in parallel. The concomitant evaluation of drug distribution between aqueous and pellet phase during *in*
200 *vitro* lipolysis and the assessment of drug permeation using the mucus-PVPA barriers was enabled by
201 the use of HTP intestinal medium, which allowed the study to be independent from the pH-stat-titration
202 apparatus typically used in the *in vitro* intestinal lipolysis model (Zangenberg et al., 2001). To account
203 for the impact that lipolysis has on *in vitro* drug distribution and on *in vitro* drug permeation, fenofibrate
204 distribution between the aqueous and pellet phase in the HTP intestinal medium and permeation across
205 the mucus-PVPA barriers were evaluated both after dispersion of SNEDDSs in the HTP intestinal
206 medium (*i.e.* absence of lipolysis) and after commencement of *in vitro* lipolysis. This evaluation allowed
207 the comparison of the data obtained in the present study with the data obtained by Michaelsen and
208 colleagues (Michaelsen et al., 2019), where *in vivo* absorption of fenofibrate was studied both while
209 lipolysis had been inhibited by the co-administration of the pancreatic lipase inhibitor orlistat, and in the
210 presence of lipolysis.

211

212 *2.2.4.1. In vitro lipolysis*

213 The three fenofibrate-loaded SNEDDSs (*i.e.* super-SNEDDS solution$_{150}$, SNEDDS$_{75}$ and super-
214 SNEDDS suspension$_{150}$) were separately weighed in a beaker and dispersed in 26 mL of HTP intestinal
215 medium (Table 2). The amount of SNEDDS (*i.e.* either super-SNEDDS solution$_{150}$, SNEDDS$_{75}$ or super-
216 SNEDDS suspension$_{150}$) added to the beaker was chosen in order to obtain a final fenofibrate
217 concentration of 480 µg/mL for all SNEDDSs and to have the same drug concentration as the one
218 utilized in the *in vitro* lipolysis experiments performed by Michaelsen and colleagues (2019). The
219 mixture was stirred at 37 °C for 20 minutes prior to the addition of the pancreatic lipase solution (4 mL)
220 in the case of the presence of lipolysis, or of HTP intestinal medium (4 ml) in the case of sole dispersion
221 (*i.e.* absence of lipolysis). To obtain the pancreatic lipase solution, the crude lipase extract was mixed
222 with 5 mL of HTP intestinal medium in the absence of calcein, and the mixture was centrifuged for 7

minutes at 6500×g. The supernatant (4 mL) was added to the beaker to initiate the lipolysis (final activity of 550 USP/mL). To simulate physiological temperature, the experiment was performed at 37 °C. Samples (1 mL), either utilized for the assessment of fenofibrate distribution in the aqueous phase or used for the permeation study, were taken out of the beaker after initial dispersion, after 30 minutes of additional dispersion or after 30 minutes from the initiation of lipolysis. This allowed to study both how the presence or absence of lipolysis affects the distribution of fenofibrate in the HTP intestinal medium on top of the mucus-PVPA barriers, and to evaluate the resulting drug permeation.

To study the distribution of fenofibrate between the aqueous and pellet phase before the start of lipolysis (*i.e.* 0 minutes) and after 30 minutes of dispersion/lipolysis, 5 µL of BBBA (1 M in MeOH) were added to the 1 mL sample to inhibit lipolysis. The inhibited samples (0 and 30 min) were exposed to centrifugation for 10 minutes at 19,000×g to allow phase separation. The concentration of fenofibrate in the aqueous phase was quantified via HPLC after dilution in MeOH, and compared to the total amount of drug in the beaker. The quantification of fenofibrate was carried out via HPLC using a Waters 2690 Separation Module HPLC system, equipped with Waters 996 Photodiode Array Detector (Waters Corporation, Milford, MA, USA) and utilizing a Phenomenex Kinetix 5u XB-C18 100A column (100 x 4.6 mm; Phenomenex, Torrance, CA, USA). The drug was detected at a wavelength of 288 nm (retention time ~ 2.5 minutes) using a mobile phase composed of 20% MilliQ water and 80% of MeOH (flow 1 mL/min). The study of fenofibrate distribution in the different phases upon lipolysis was carried out in triplicate for each SNEDDS.

To confirm that the pH conditions were kept constant during dispersion/lipolysis by the buffering capacity of the HTP intestinal medium, the pH was monitored using a SensION^{TM} PH 31 pH meter (HACH, Dusseldorf, Germany). Moreover, the size of the SNEDDSs droplets after dispersion and after initiation of lipolysis was determined using a Malvern Zetasizer Nano ZS (Malvern, Oxford, UK). Samples were prepared by dispersing the SNEDDS pre-concentrate in HTP intestinal medium (concentration 1.45 mg/mL), and for the investigation on the effect of lipolysis on the droplet size, pancreatic lipase extract was added to the dispersion in order to obtain a final activity of 550 USP/mL. The operating conditions used for the size determination were the following: viscosity of the sample

dispersant 0.8872 cP, temperature 25.0 ºC, measurement angle 173 º backscatter, cell type disposable cuvettes (DTS0012), number of measurements 3.

2.2.4.2. In vitro permeation

To study the permeation of fenofibrate from the different SNEDDSs, samples (1 mL) were taken out of the beaker before the start of lipolysis (*i.e*. sole dispersion, absence of lipolysis) and right after initiation of lipolysis (*i.e.* after the addition of the pancreatic extract), and were transferred (100 µL) on top of the mucus-PVPA barriers. The samples where lipolysis was initiated (100 µL) were transferred on top of the mucus-PVPA barriers without inhibiting lipolysis, thus allowing this process to continue on top of the barriers. The mucus-PVPA barriers were then placed in acceptor Transwell wells containing 600 µL of acceptor medium and the permeation experiment was carried out at 37 °C for a total of 6 hours. DMSO 40 mg/mL in phosphate buffered saline (PBS) pH 7.4 was chosen as the acceptor medium to both simulate the pH conditions of the systemic blood circulation and to enable higher fenofibrate solubility compared to PBS pH 7.4 (Falavigna et al., 2020a). Higher fenofibrate solubility in the acceptor medium resulting from the presence of DMSO allows a higher amount of drug to permeate and this aids in the quantification of the permeated drug (Falavigna et al., 2020a). The barriers were moved to wells containing fresh acceptor medium after 2, 4 and 6 hours to maintain sink conditions. At the end of the permeation experiment, samples (200 µL) from the acceptor compartments were taken out to quantify the amount of fenofibrate permeated over time.

As the previous assessment of the compatibility of the PVPA barriers with the components in the donor compartment showed that the presence of BM was essential for the correct functionality of the barriers (Falavigna et al., 2020a), BM was placed on top of the PVPA barriers in all of the permeation experiments. Moreover, in the present study, to assure the correct functionality of the mucus-PVPA barriers during the permeation experiment, an in-line assessment of barrier integrity was carried out in parallel to the fenofibrate permeation study. This evaluation was done by measuring the permeability of calcein contained in the HTP intestinal medium and the electrical resistance across the barriers at the

end of the permeation study. To this regard, it has been demonstrated that high calcein permeability (> $0.06 * 10^{-6}$ cm/s) and low electrical resistance (< 290 Ohm * cm^2) indicate barrier impairment (Falavigna et al., 2018; Falavigna et al., 2019).

The quantification of fenofibrate was carried out at 288 nm using the spectrophotometer module of the Spark Multimode Microplate Reader (Tecan, Männendorf, Switzerland), while calcein was quantified using the spectrofluorometer module of the same apparatus at excitation wavelength of 485 nm and emission of 520 nm.

Calcein apparent permeability (*i.e.* P_{app}) was calculated following the equation:

$$P_{app}\left(\frac{cm}{s}\right) = \frac{dQ}{dt} * \frac{1}{A * Cd}$$

Where *dQ/dt* is the flux at the steady state (nmol/s), *A* expresses the surface area of the PVPA barriers (0.33 cm^2) and C_d is the calcein concentration in the donor compartment at time zero (nmol/mL).

All permeability experiments were conducted using a total of 12 PVPA barriers.

2.2.5. In vivo-in vitro correlation

The areas under the curve (AUCs) resulting from the *in vivo* plasma concentration of fenofibrate in rats obtained by Michaelsen and colleagues (Michaelsen et al., 2019) for the three SNEDDSs (*i.e.* super-SNEDDS $solution_{150}$, $SNEDDS_{75}$ and super-SNEDDS $suspension_{150}$) were compared to the AUC resulting from either i) the *in vitro* dispersion/lipolysis described in Section 2.2.4.1, or ii) the *in vitro* permeation data described in Section 2.2.4.2. The *in vitro* dispersion/lipolysis/permeation AUC was calculated using GraphPad Prism 8.4.1 (GraphPad Software, San Diego, CA, USA) by utilizing a linear trapezoidal model from t = 0 to t = 30 min/6 h. For the calculation of the AUC resulting from *in vitro* dispersion/lipolysis, the amount of fenofibrate found in the aqueous phase upon lipolysis over time was utilized. The AUCs of the *in vitro* permeation study was obtained from the mass transfer of fenofibrate permeated across the mucus-PVPA barriers over time. This comparison allowed to determine the IVIVC between the above-mentioned sets of data, and to study if the *in vitro* dispersion/lipolysis or combined

dispersion/lipolysis/permeation data could predict *in vivo* drug absorption for the investigated SNEDDSs.

2.2.6. Statistical analysis

GraphPad Prism 8.4.1 (GraphPad Software, San Diego, CA, USA) was used for the statistical analysis of the results obtained in this study. One-way ANOVA was used to compare three or more sets of data, followed by Šidák *post hoc* test to determine significant difference between results ($p < 0.05$).

3. Results and discussion

In the present study, the need for a combined *in vitro* lipolysis-permeation model able to predict *in vivo* drug absorption from SNEDDSs was met by the combination of the HTP *in vitro* lipolysis model with the mucus-PVPA *in vitro* permeation model. In particular, the HTP *in vitro* lipolysis model allowed a simple and pH-stat-titration-independent evaluation of fenofibrate distribution in the aqueous and pellet phase after dispersion or lipolysis of three SNEDDSs, whereas the mucus-PVPA model allowed the evaluation of fenofibrate permeation. Finally, *in vitro* drug solubilization and drug permeation data were separately compared to *in vivo* absorption data present in the literature (Michaelsen et al., 2019) to assess the prediction potential of the experimental setups utilized in this study. The Level D correlation between *in vivo* and *in vitro* data was therefore determined since it is considered as a useful qualitative correlation that can be utilized during formulation development (Shen and Burgess 2015).

3.1. Effect of in vitro lipolysis of SNEDDSs on fenofibrate distribution

The distribution of fenofibrate between the aqueous and pellet phase was studied after addition of the three SNEDDSs to the HTP intestinal medium both in the absence (*i.e.* sole dispersion) and presence of *in vitro* lipolysis for a total of 30 minutes. This investigation was carried out to estimate i) how much of the drug would be found in the aqueous phase over time (*i.e.* amount of drug potentially available for

absorption) ii) which SNEDDS would result in a better drug solubilization upon dispersion/lipolysis and iii) how the presence of lipolysis affects the drug distribution between the aqueous and pellet phase compared to the absence of lipolysis. Moreover, the pH in the presence of *in vitro* lipolysis was measured to assure that the optimal pH condition for the activity of the pancreatic lipase would be maintained (*i.e.* pH ~ 6.5). In fact, the activity of the pancreatic enzyme has shown to induce the release of fatty acids upon digestion of SNEDDS, resulting in a decrease in pH and thus inhibition of the lipolysis process (Zangenberg et al., 2001). To this regard, the HTP intestinal medium proved to be able to keep the pH around 6.48 ± 0.03 thanks to its high buffer capacity throughout all *in vitro* lipolysis experiments, in accordance with the results from Mosgaard and colleagues (Mosgaard et al., 2015). This pH condition was also kept in the absence of lipolysis, thus enabling the comparison between the drug distribution in the presence and absence of lipolysis.

As can be observed in Fig. 1, both in the absence (Fig. 1A) and presence (Fig. 1B) of lipolysis, $SNEDDS_{75}$ was able to maintain most of the drug solubilized in the aqueous phase during 30 minutes of dispersion/lipolysis. However, for both super-$SNEDDS\ solution_{150}$ and super-$SNEDDS\ suspension_{150}$ the absence and presence of lipolysis both caused precipitation of the drug, thus increasing the amount found in the pellet phase ~~especially in the case of super-$SNEDDS\ suspension_{150}$~~. The same trend has previously been observed, where super-$SNEDDS\ solution_{150}$ caused higher fenofibrate precipitation over time than $SNEDDS_{75}$ and lower precipitation than super-$SNEDDS\ suspension_{150}$ (Falavigna et al., 2020a). Notably, in the presence of lipolysis drug precipitation occurred to a greater extent from 0 to 30 minutes in the case of super-$SNEDDS\ solution_{150}$ compared to super-$SNEDDS\ suspension_{150}$ (Figure 1B). In fact, a modest change in precipitation was observed for super-$SNEDDS\ suspension_{150}$, while for super-$SNEDDS\ solution_{150}$ this change was more drastic, most likely due to the instability of the supersaturated system resulting from this formulation.

While drug precipitation in the pellet phase significantly increased over time ($p < 0.05$) in the presence of lipolysis (Fig. 1B) for super-$SNEDDS\ solution_{150}$ and super-$SNEDDS\ suspension_{150}$, ~~whereas~~ after 30 minutes of dispersion (*i.e.* absence of lipolysis) the amount of drug found in the pellet phase was the same as at the start of the experiment (Fig. 1A). This trend was also found in the study by Michaelsen and colleagues (Michaelsen et al., 2019), where fenofibrate distribution between the aqueous and pellet

phase of the same SNEDDSs was evaluated in two conditions, i) inhibition of dynamic *in vitro* lipolysis by the use of the pancreatic lipase inhibitor orlistat and ii) the presence of dynamic *in vitro* intestinal lipolysis. Further, the precipitation of fenofibrate remained constant in the presence of the pancreatic lipase inhibitor, whereas in its absence (*i.e.* active lipolysis) drug precipitation increased over time for super-SNEDDS solution$_{150}$ and super-SNEDDS suspension$_{150}$ (Michaelsen et al., 2019). The increase in drug precipitation upon *in vitro* lipolysis is to be expected as the addition of the pancreatic lipase can induce the formation of different colloidal structures (*i.e.* micelles and vesicles) which are able to solubilize the incorporated drug to a different extent compared to the nano-emulsion droplets of the SNEDDSs obtained after dispersion in the HTP intestinal medium (Mosgaard et al., 2015). To this regard, the size of the SNEDDSs droplets was determined after dispersion and after initiation of lipolysis. The results showed that the SNEDDSs diameter after dispersion was around 50.89 ± 1.09 nm with a polydispersity index of 0.38, suggesting a rather monodispersed size distribution, whereas after initiation of lipolysis it was not possible to determine the size of the SNEDDSs due to a highly polydispersed size population (polydispersity index > 0.8), suggesting the formation of structures with various sizes upon the initiation of lipolysis. The structural changes in ~~different size of~~ the colloidal ~~structures~~ species formed after dispersion compared to after lipolysis could have an effect on drug precipitation, and could be the underlying cause for the differences in drug solubilization shown in Fig. 1.

The results discussed thus far confirm the correct functionality of the HTP intestinal medium in maintaining the desired pH condition for the *in vitro* lipolysis process, and highlight the similarity of the obtained results with already published data. The use of the HTP intestinal medium eliminates the need for the pH-stat-titration typically used in the *in vitro* intestinal lipolysis method, resulting in a simpler and less apparatus-dependent model.

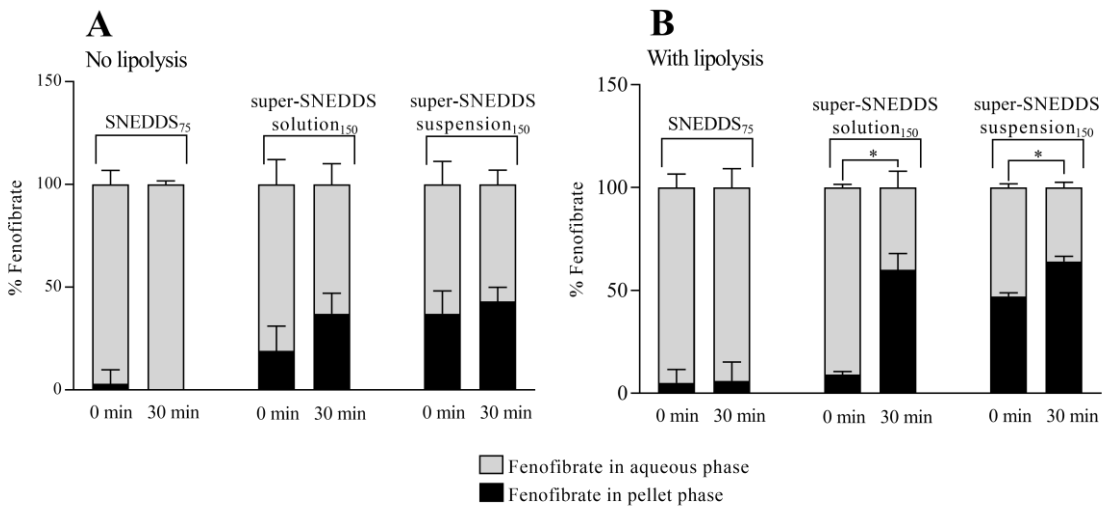

Fig. 1: Fenofibrate (%) present in the pellet (black) and aqueous phase (grey) over time A) in the absence of lipolysis (*i.e.* sole dispersion) and B) with lipolysis for $SNEDDS_{75}$, super-$SNEDDS\ solution_{150}$ and super-$SNEDDS\ suspension_{150}$. (Mean ± SD; n = 3). *Statistically significant ($p < 0.05$) difference between the percentages of fenofibrate in the aqueous phase after 0 minutes compared to 30 minutes.

3.2. In vitro permeation of fenofibrate

The permeation of fenofibrate across the mucus-PVPA barriers was determined both in the absence (*i.e.* sole dispersion) and presence of lipolysis to determine i) which SNEDDS would enable the highest drug mass transfer across the barriers and ii) whether the presence of lipolysis would cause a change in mass transfer compared to its absence. In parallel to the estimation of fenofibrate mass transfer, an in-line assessment of barrier integrity was carried out by measuring the permeability of the highly hydrophilic marker calcein and by determining the electrical resistance across the mucus-PVPA barriers at the end of the permeation experiment. As can be observed in Table 3, the barriers maintained their integrity in all of the tested conditions, as values of calcein P_{app} and electrical resistance were within the limits previously associated to barrier integrity (*i.e.* calcein $P_{app} < 0.06 \cdot 10^{-6}$ cm/s and electrical resistance > 290 Ohm · cm^2 (Falavigna et al., 2018))

	SNEDDS	Calcein P_{app} (10^{-6} cm/s)	Electrical resistance (Ω cm^2)
No lipolysis (dispersion)	Super-SNEDDS solution$_{150}$	0.050 ± 0.017	422 ± 22
	SNEDDS$_{75}$	0.055 ± 0.002	373 ± 8
	Super-SNEDDS suspension$_{150}$	0.057 ± 0.011	450 ± 3
With lipolysis	Super-SNEDDS solution$_{150}$	0.023 ± 0.005	562 ± 37
	SNEDDS$_{75}$	0.027 ± 0.001	541 ± 5
	Super-SNEDDS suspension$_{150}$	0.018 ± 0.004	818 ±112

Table 3: Calcein P_{app} and the electrical resistance across the mucus-PVPA barriers during dispersion/lipolysis-permeation experiments. (Mean ± SD; n = 12).

In terms of fenofibrate mass transfer across the mucus-PVPA barrier, both in the absence (Fig. 2A) and presence (Fig. 2B) of lipolysis, super-SNEDDS solution$_{150}$ exhibited the highest fenofibrate mass transfer, suggesting that this formulation would lead to the highest bioavailability in both cases. Instead, for SNEDDS$_{75}$ and super-SNEDDS suspension$_{150}$ the ranking was different according to the absence or presence of lipolysis; in fact, super-SNEDDS suspension$_{150}$ promoted a significantly higher mass transfer of fenofibrate in the absence of lipolysis compared to SNEDDS$_{75}$, whereas in its presence SNEDDS$_{75}$ and super-SNEDDS suspension$_{150}$ led to a similar drug permeation across the mucus-PVPA barriers (Fig. 2).

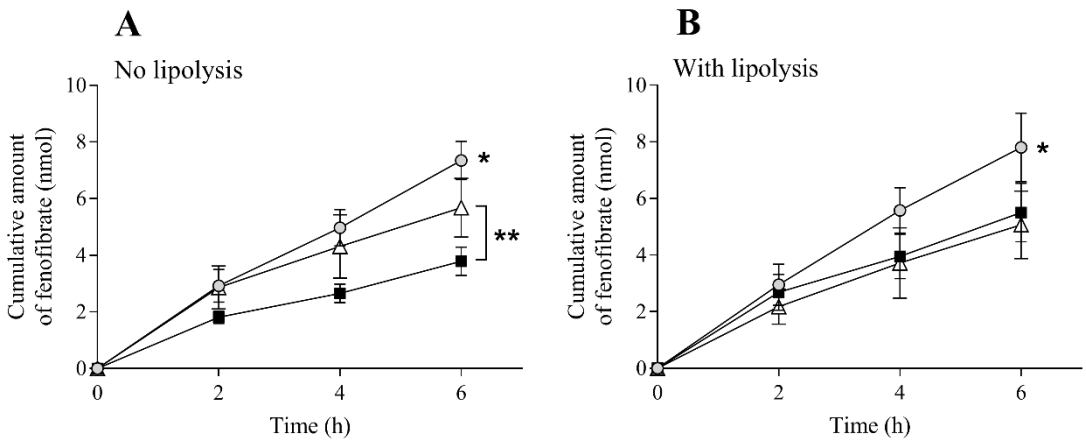

409

410 **Fig. 2:** Fenofibrate permeated across the mucus-PVPA barriers (cumulative amount) from super-
411 SNEDDS solution$_{150}$ (grey circle), SNEDDS$_{75}$ (black square) and super-SNEDDS suspension$_{150}$ (white
412 triangle) A) in the absence of lipolysis and B) with lipolysis. (Mean ± SD; n = 12). *Statistically
413 significant ($p < 0.05$) difference between the amount of fenofibrate permeated from super-SNEDDS
414 solution$_{150}$ and from super-SNEDDS suspension$_{150}$ and SNEDDS$_{75}$. **Statistically significant ($p < 0.05$)
415 difference between the amount of fenofibrate permeated from super-SNEDDS suspension$_{150}$ and
416 SNEDDS$_{75}$.

417

418 The change in ranking in terms of fenofibrate plasma concentration was also observed by Michaelsen
419 and colleagues (Michaelsen et al., 2019), where the same SNEDDSs were administered to rats both in
420 the presence of lipolysis and after this process was inhibited by the co-administration of the pancreatic
421 lipase inhibitor orlistat. The authors found that the absorption of fenofibrate from super-SNEDDS
422 suspension$_{150}$ significantly increased when orlistat was present. Regarding this, it was suggested that
423 when lipolysis is inhibited, the SNEDDS nano-emulsion droplets remain present in the GI tract,
424 providing constant solubilization of the drug and aid in the drug absorption process while avoiding
425 further precipitation (Michaelsen et al., 2019). The positive effect of the absence of lipolysis on drug
426 solubilization can also be observed in Fig. 1A, where fenofibrate precipitation did not increase over time
427 in the absence of lipolysis, whereas when this process was initiated, drug precipitation increased (Fig.
428 1B). Therefore, in the case of the super-SNEDDS suspension$_{150}$ for both this study and the one from

Michaelsen and colleagues (Michaelsen et al., 2019) the inhibition of lipolysis maintained fenofibrate solubilized for a longer time. However, it has to be noted that the drug found in the aqueous phase is present as both solubilized in the SNEDDS nano-emulsion droplets/in the colloidal structures formed upon lipolysis and free in solution. The ability to keep the drug free in solution promotes drug permeation, as only this fraction is able to cross the permeation barrier (Keemink and Bergström, 2018). In the current study, a difference in drug transfer between the absence and presence of lipolysis was also observed for $SNEDDS_{75}$, where drug permeation was found to be higher in the presence of lipolysis. In contrast to the super-SNEDDS $suspension_{150}$, where fenofibrate is present both as a precipitate and solubilized in the SNEDDS, the $SNEDDS_{75}$ has all the drug completely solubilized in the nano-emulsion droplets. Thus, when $SNEDDS_{75}$ is dispersed in the HTP intestinal medium most of the drug is possibly solubilized in the SNEDDS, rather than free in solution. The formation of different colloidal structures upon *in vitro* lipolysis can shift the equilibrium of the drug towards the fraction free in solution, translating to higher fenofibrate permeation in the presence of lipolysis. The increase in fenofibrate permeation in the presence of lipolysis for $SNEDDS_{75}$ was not observed in the previous study (Falavigna et al., 2020a), as it was found that $SNEDDS_{75}$ had similar fenofibrate permeation both in the absence and presence of lipolysis. Differences in fenofibrate permeation between published data and the results collected in the present study could be due to the different compositions of the utilized simulated intestinal fluids. In fact, in the case of HTP intestinal medium, the high concentration of Bis-Tris might affect i) the droplet size of the SNEDDSs and of the colloidal structures forming upon lipolysis, ii) the drug equilibrium between the fraction free in solution and the one solubilized by the SNEDDS and iii) the extent and nature of drug precipitate, thus possibly leading to a change in drug permeation. Moreover, it has to be noted that drug solubilization in SNEDDSs in the absence of drug supersaturation or precipitation can reduce the drug thermodynamic activity (Yeap et al., 2013), and it has been demonstrated that drug solubilization in SNEDDSs does not lead to higher drug absorption if the free drug concentration does not increase, despite the rise in total solubilized drug (Yeap et al., 2013). On the other hand, drug supersaturation can result in an increase in thermodynamic activity and instability, possibly resulting in drug precipitation (Tanaka et al., 2020), as suggested by the results described in Section 3.1 with regards to super-SNEDDS $solution_{150}$ and super-SNEDDS $suspension_{150}$ (Fig. 1).

However, drug precipitation caused by the thermodynamic instability of a supersaturated state does not necessarily translate to lower drug absorption, as the solid state of the precipitate could re-dissolve and thus lead to high absorption (Tanaka et al., 2020). However, to confirm the hypothesis that fenofibrate could re-dissolve from its precipitated state and to identify the mechanisms behind this process, further characterization of the drug and SNEDDSs would be needed.

3.3. In vivo-in vitro correlation

The results obtained in this study and described in Section 3.1 and 3.2 were compared to the ones obtained by Michaelsen and colleagues (Michaelsen et al., 2019), where the same SNEDDSs were utilized to study fenofibrate absorption in rats. In particular, the AUCs resulting from the *in vivo* study, where lipolysis was either inhibited (-) by presence of orlistat or taking place (+) ($AUC_{in\ vivo,\ -/+\ lipolysis}$), were compared to the AUCs resulting from the amount of drug found in the aqueous phase after *in vitro* dispersion (-) or lipolysis (+) over time ($AUC_{in\ vitro,\ -/+\ lipolysis}$). The same *in vivo* data was also compared to the AUCs calculated from the fenofibrate mass transfer after *in vitro* permeation in the absence (-) or presence (+) of lipolysis using the mucus-PVPA barriers ($AUC_{in\ vitro\ permeation,\ -/+\ lipolysis}$) (Table 4). Moreover, the statistical difference in AUC between absence and presence of lipolysis for both *in vivo* and *in vitro* results was evaluated (Table 4), and the IVIVC between these sets of data were determined (Fig. 3 and Fig. 4).

	Super-SNEDDS solution$_{150}$	SNEDDS$_{75}$	Super-SNEDDS suspension$_{150}$
In vivo $AUC_{0\text{-}30h,\ -\ lipolysis}$ (μg·h/mL)	136.9 ± 27.5	66.3 ± 14.9	108.9 ± 39.5
In vivo $AUC_{0\text{-}30h,\ +\ lipolysis}$ (μg·h/mL)	148.0 ± 47.5	88.3 ± 20.9	58.1 ± 16.9
In vitro $AUC_{0\text{-}0.5\ h,\ -\ lipolysis}$ (min·%)	2160.0 ± 235.8	2985.0 ± 105.4	1800.0 ± 197.1
In vitro $AUC_{0\text{-}0.5\ h,\ +\ lipolysis}$ (min·%)	1965.0 ± 121.5	2835.0 ± 168.5	1335.0 ± 46.1

In vitro $AUC_{0\text{-}6\ h\ permeation,\ -\ lipolysis}$ (nmol·h)	23.0 ± 1.4	13.0 ± 0.8	20.0 ± 2.2
In vitro $AUC_{0\text{-}6\ h\ permeation,\ +\ lipolysis}$ (nmol·h)	25.0 ± 2.0	19.0 ± 1.8	17.0 ± 2.3

Table 4: Area under the curve (AUC) resulting from fenofibrate absorption from *in vivo* studies in rats in the absence (-) or presence (+) of lipolysis (Michaelsen et al., 2019) (*in vivo* $AUC_{0\text{-}30\ h,\ -/+\ lipolysis}$), AUC from drug solubilization without (-) and with (+) *in vitro* lipolysis (*i.e.* amount of drug found in the aqueous phase; *in vitro* $AUC_{0\text{-}0.5\ h,\ -/+\ lipolysis}$) and mass transfer of fenofibrate permeated across the mucus-PVPA barriers without (-) or with (+) lipolysis (*in vitro* $AUC_{0\text{-}6\ h\ permeation,\ -/+\ lipolysis}$) from super-SNEDDS $solution_{150}$, $SNEDDS_{75}$ and super-SNEDDS $suspension_{150}$. (Mean ± SEM; n = 6).

3.3.1. Correlation with in vitro drug solubilization upon dispersion/lipolysis

As can be observed in Fig. 3 and Table 4, the *in vitro* solubilization data ($AUC_{0\text{-}0.5\ h,\ -/+\ lipolysis}$) failed to correlate with *in vivo* plasma concentration in rats both in the absence and presence of lipolysis. In fact, the prediction of drug absorption *via* the evaluation of drug found in the aqueous phase during dispersion/lipolysis does not take into account that the fenofibrate present in the aqueous phase is in a dynamic equilibrium between its fraction freely dissolved in the luminal contents and the fraction solubilized by the SNEDDS colloidal structures formed upon lipolysis. Therefore, the drug in the aqueous phase is an overestimation of the amount of drug freely solubilized and thus available for permeation (Michaelsen et al., 2019). This was clearly evident when $SNEDDS_{75}$ was evaluated. In fact, according to the drug distribution in the aqueous and pellet phase after dispersion/lipolysis ($AUC_{0\text{-}0.5\ h,\ -/+\ lipolysis}$), $SNEDDS_{75}$ is the one where most of the drug is found in the aqueous phase (Fig. 1, Table 4), whereas *in vivo* the corresponding AUC is lower than for the super-SNEDDS $solution_{150}$. The difference in the ranking between the *in vitro* dispersion/lipolysis and *in vivo* plasma concentration data can be ascribed to the above-mentioned lack of distinction between the freely solubilized drug and the drug in

the colloidal structures, and also to the lack of an absorption step. In fact, Bevernage and colleagues (Bevernage et al., 2012) have evaluated the influence of an absorption step on supersaturation and precipitation of a poorly water-soluble drug, and found that precipitation from a supersaturated system can be suppressed by the escape of the drug *via* the absorption sink, thus averting the system from reaching a critical degree of supersaturation and the start of precipitation. Thus, the results described in the study by Bevernage and colleagues (Bevernage et al., 2012) suggest that precipitation kinetics change when supersaturated drugs have the chance of permeating instead of precipitating, and that the shift towards drug permeation instead of precipitation increases with increasing degrees of supersaturation.

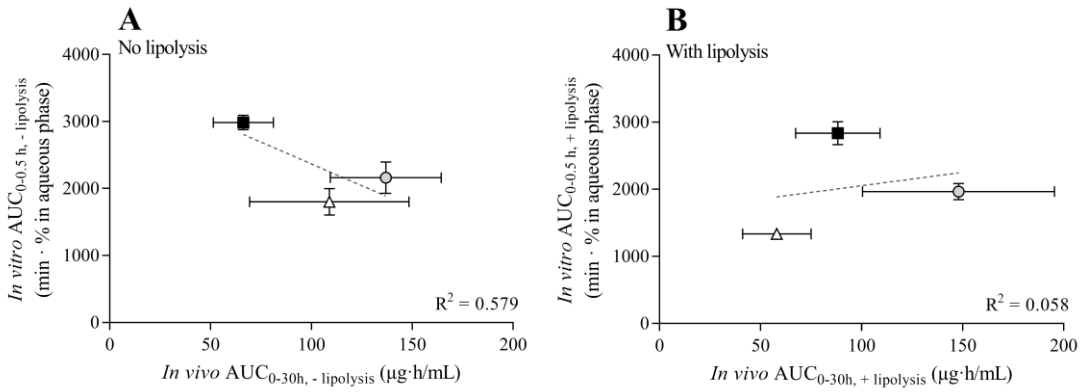

Fig. 3: IVIVC between *in vivo* plasma exposure (Michaelsen et al., 2019) and *in vitro* fenofibrate solubilization (*i.e.* amount of drug in the aqueous phase) of super-SNEDDS solution$_{150}$ (grey circle), SNEDDS$_{75}$ (black square) and super-SNEDDS suspension$_{150}$ (white triangle) A) in the absence (-) of lipolysis and B) with (+) lipolysis.

3.3.2. Correlation with in vitro drug permeation

The results depicted in Fig. 4, where the AUCs resulting from the *in vitro* permeation of fenofibrate ($AUC_{0\text{-}6\ h\ permeation,\ -/+\ lipolysis}$) were plotted against the *in vivo* drug absorption data ($AUC_{0\text{-}30\ h,\ -/+\ lipolysis}$), are proof of the importance of the absorption step in *in vitro* models evaluating lipid-based formulations,

(Fig. 4). In fact, an excellent IVIVC ($R^2 > 0.98$) was found when comparing the *in vitro* drug permeation in the absence or presence of lipolysis with *in vivo* data where lipolysis was either inhibited (*i.e.* use of orlistat) or taking place. The lack of IVIVC using *in vitro* drug distribution data from the dispersion/lipolysis experiments alone ($AUC_{0\text{-}0.5\ h,\ -/+\ lipolysis}$) (Fig. 3) compared to the good correlation obtained using the *in vitro* permeation data following dispersion/permeation (Fig. 4) suggests that the intrinsic solubilization of SNEDDSs does not dictate the degree of drug absorption, whereas the propensity of SNEDDSs to promote supersaturation seems to be more important (Yeap et al., 2013).

Moreover, the presence of the mucus layer on top of the mucosa of the small intestine has been suggested to play an important role in stabilizing drug supersaturation. In fact, it has been found that mucin and pig intestinal mucus were both able to delay precipitation during supersaturation-permeation experiments for two PWSD (Yeap et al., 2019). It has been proposed that the mechanisms enabling the stabilization of supersaturation exerted by the mucus layer were drug-specific. In particular, it has been shown that the presence of mucin and pig intestinal mucus delayed carvedilol and piroxicam precipitation, and that the absorption of carvedilol from a supersaturated solution was higher across mucus-producing co-culture of Caco-2 cell-layers compared to non-mucus-producing ones (Yeap et al., 2019). Therefore, the absence of biosimilar mucus in the HTP dispersion/lipolysis setup (Section 3.1) could be another reason why the *in vitro* lipolysis evaluation did not correlate with *in vivo* data, as the stabilization of drug supersaturation could not be carried out by the mucus layer. During the *in vitro* permeation experiments, on the other hand, the biosimilar mucus layer lining the PVPA barriers possibly enabled the maintenance of fenofibrate supersaturation by delaying drug precipitation, and thus leading to higher mass transfer for those formulations providing a supersaturated fenofibrate concentration (*i.e.* super-SNEDDS $solution_{150}$ and super-SNEDDS $suspension_{150}$). The good IVIVC obtained using the mucus-PVPA model (Fig. 4) together with the results described by Yeap and colleagues (Yeap et al., 2019) highlight the importance of having a mucus layer lining the permeation barrier when studying the permeation of supersaturated PWSD. This is especially relevant as the supersaturation stabilization process could be seen as an intrinsic mechanism of action for lipid-based formulations, and it should thus be taken into consideration in the development of novel drug delivery systems.

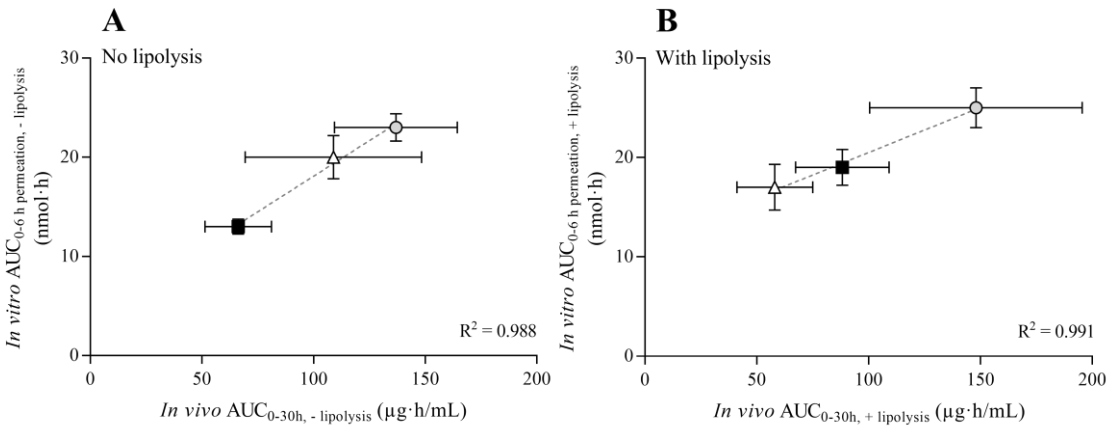

Fig. 4: IVIVC between *in vivo* plasma exposure (Michaelsen et al., 2019) and *in vitro* fenofibrate permeation across the mucus-PVPA barriers A) in the absence (-) of lipolysis and B) with (+) lipolysis from super-SNEDDS solution$_{150}$ (grey circle), SNEDDS$_{75}$ (black square) and super-SNEDDS suspension$_{150}$ (white triangle).

Overall, the results presented in this study underline the complexity of the processes affecting the performance of SNEDDSs *in vivo*, and emphasize that drug solubilization, supersaturation, precipitation and permeation all coexist in a dynamic equilibrium that drives drug absorption. This could be simulated with the use of an appropriate *in vitro* model as the one presented in this work. Further studies assessing a broader selection of drugs and formulations need to be performed to investigate the full potential of the combined *in vitro* model developed in this study. At this stage, this appears to be a very promising approach to estimate *in vivo* performance of lipid-based formulations, and as such a highly valuable tool in the development and optimization of this type of formulations.

4. Conclusion

The obtained results demonstrate that the present study succeeded in the development of a combined *in vitro* lipolysis-permeation model able to predict *in vivo* drug absorption from the investigated

SNEDDSs. The typical *in vitro* intestinal lipolysis model was substituted with the HTP *in vitro* lipolysis model to allow the use of a pH-stat-titration-independent system and permit the simultaneous investigation of *in vitro* lipolysis and permeation. While no correlation was found when comparing the amount of drug solubilized in the aqueous phase upon *in vitro* dispersion/lipolysis with the *in vivo* literature data (Michaelsen et al., 2019) ($R^2 < 0.58$), the addition of an *in vitro* permeation step using the mucus-PVPA barriers led to excellent IVIVCs ($R^2 > 0.98$). Also, the difference in fenofibrate *in vivo* absorption between the presence and absence of lipolysis could be accurately predicted by the combined *in vitro* model. Herewith, the evidence gathered in this study suggests that the evaluation of *in vitro* drug distribution alone cannot predict drug plasma concentration *in vivo*, while the combination with *in vitro* drug permeation assessed with the use of the mucus-PVPA model is able to do so to a higher extent. The combined *in vitro* model presented in this study could thus be a highly valuable tool in the development and optimization of novel lipid-based formulations.

Acknowledgements

The authors thank UiT The Arctic University of Norway for funding PhD student Margherita Falavigna and Lipoid GmbH (Ludwigshafen, Germany) for the donation of phospholipids. NordicPOP (supported by NordForsk for the Nordic University Hub project number: 85352), and COST Action UNGAP (supported by the European Cooperation in Science and Technology; project number: 16205) are highly acknowledged for enabling fruitful collaboration.

Funding

This research did not receive any specific grant from funding agencies in the public, commercial, or not-for-profit sectors.

Conflict of interest

The authors confirm no conflicts of interest.

References:

Alskär LC, Parrow A, Keemink J, Johansson P, Abrahamsson B, Bergström CAS. Effect of lipids on absorption of carvedilol in dogs: Is coadministration of lipids as efficient as a lipid-based formulation? J. Control. Release 2019; 304: 90-100. https://doi.org/10.1016/j.jconrel.2019.04.038

Artursson P, Palm K, Luthman K. Caco-2 monolayers in experimental and theoretical predictions of drug transport. Adv. Drug Deliv. Rev. 2001; 46: 27–43. https://doi.org/10.1016/s0169-409x(00)00128-9

Berben P, Brouwers J, Augustijns P. Assessment of passive intestinal permeability using an artificial membrane insert system. J. Pharm. Sci. 2018; 107: 250–256. https://doi.org/10.1016/j.xphs.2017.08.002

Berthelsen R, Klitgaard M, Rades T, Müllertz A. In vitro digestion models to evaluate lipid based drug delivery systems; present status and current trends. Adv. Drug Deliv. Rev. 2019; 142: 35-49. https://doi.org/10.1016/j.addr.2019.06.010

Bevernage J, Brouwers J, Annaert P, Augustijns P. Drug precipitation–permeation interplay: Supersaturation in an absorptive environment. Eur. J. Pharm. Biopharm. 2012; 82: 424-428. https://doi.org/10.1016/j.ejpb.2012.07.009

Bibi HA, Holm R, Bauer-Brandl A. Simultaneous lipolysis/permeation in vitro model, for the estimation of bioavailability of lipid based drug delivery systems. Eur. J. Pharm. Biopharm. 2017; 117: 300–307. https://doi.org/10.1016/j.ejpb.2017.05.001

Boegh M, Baldursdóttir SG, Müllertz A, Nielsen HM. Property profiling of biosimilar mucus in a novel mucus-containing in vitro model for assessment of intestinal drug absorption. Eur. J. Pharm. Biopharm. 2014; 87: 227-235. https://doi.org/10.1016/j.ejpb.2014.01.001

612 Dahlgren D, Lennernäs H. Intestinal Permeability and Drug Absorption: Predictive Experimental,
613 Computational and In Vivo Approaches. Pharmaceutics 2019; 11 (8): 411.
614 https://doi.org/10.3390/pharmaceutics11080411

615 di Cagno M, Bibi HA, Bauer-Brandl A. New biomimetic Permeapad™ for efficient investigation of
616 passive permeability of drugs. Eur. J. Pharm. Sci. 2015; 73: 29–34.
617 https://doi.org/10.1016/j.ejps.2015.03.019

618 Falavigna M, Klitgaard M, Berthelsen R, Müllertz A, Flaten GE. Predicting oral absorption of
619 fenofibrate in lipid-based drug delivery systems by combining in vitro lipolysis with the mucus-PVPA
620 permeability model, J. Pharm. Sci. 2020a. https://doi.org/10.1016/j.xphs.2020.08.026

621 Falavigna M, Klitgaard M, Brase C, Ternullo S, Skalko-Basnet N, Flaten GE. Mucus-PVPA (mucus
622 phospholipid vesicle-based permeation assay): an artificial permeability tool for drug screening and
623 formulation development. Int. J. Pharm. 2018; 537: 213–222.
624 https://doi.org/10.1016/j.ijpharm.2017.12.038

625 Falavigna M, Klitgaard M, Steene E, Flaten GE. Mimicking regional and fasted/fed state conditions in
626 the intestine with the mucus-PVPA in vitro model: The impact of pH and simulated intestinal fluids on
627 drug permeability. Eur. J. Pharm. Sci. 2019; 132: 44-54. https://doi.org/10.1016/j.ejps.2019.02.035

628 Falavigna M, Stein PC, Flaten GE, Pio di Cagno M. Impact of Mucin on Drug Diffusion: Development
629 of a Straightforward in Vitro Method for the Determination of Drug Diffusivity in the Presence of
630 Mucin. Pharmaceutics 2020b; 12 (168): 1-13. https://doi.org/10.3390/pharmaceutics12020168

631 Feeney OM, Crum MF, McEvoy CL, Trevaskis NL,Williams HD, Pouton CW, Charman WN,
632 Bergström CAS, Porter CJH. 50 years of oral lipid-based formulations: Provenance, progress and future
633 perspectives. Adv. Drug Deliv. Rev. 2016; 101: 167-194. https://doi.org/10.1016/j.addr.2016.04.007

634 Flaten GE, Dhanikula AB, Luthman K, Brandl M. Drug permeability across a phospholipid vesicle
635 barrier: a novel approach for studying passive diffusion. Eur. J. Pharm. Sci. 2006; 27: 80–90.
636 https://doi.org/10.1016/j.ejps.2005.08.007

637 Gao P, Morozowich W. Development of supersaturatable self-emulsifying drug delivery system
638 formulations for improving the oral absorption of poorly soluble drugs. Expert opinion on drug delivery
639 2006; 3 (1): 97–110. https://doi.org/10.1517/17425247.3.1.97

640 Hedge OJ, Bergström CAS. Suitability of ArtificialMembranes in Lipolysis-Permeation Assays of Oral
641 Lipid-Based Formulations. Pharm. Res. 2020; 37:99. https://doi.org/10.1007/s11095-020-02833-9

642 Ille AR, Griffin BT, Brandl M, Bauer-Brandl A, Jacobsen AC, Vertzoni M, Kuentz M, Kolakovic R,
643 Holm R. Exploring impact of supersaturated lipid-based drug delivery systems of celecoxib on in vitro
644 permeation across Permeapad® membrane and in vivo absorption. Eur. J. Pharm. Sci. 2020; 152:
645 105452. https://doi.org/10.1016/j.ejps.2020.105452

646 Kansy M, Senner F, Gubernator K. Physicochemical high throughput screening: parallel artificial
647 membrane permeation assay in the description of passive absorption processes. J. Med. Chem.1998; 41:
648 1007–1010. https://doi.org/10.1021/jm970530e

649 Keemink J, Bergström CAS. Caco-2 cell conditions enabling studies of drug absorption from digestible
650 lipid-based formulations. Pharm. Res. 2018; 35: 74. https://doi.org/10.1007/s11095-017-2327-8

651 Keemink J, Mårtensson E, Bergström CAS. Lipolysis-Permeation setup for simultaneous study of
652 digestion and absorption in vitro. Mol. Pharm. 2019; 16: 921-930.
653 https://doi.org/10.1021/acs.molpharmaceut.8b00811

654 Lechanteur A, das Neves J, Sarmento B. The role of mucus in cell-based models used to screen mucosal
655 drug delivery. Adv. Drug Deliv. Rev. 2018; 124: 50-63. https://doi.org/10.1016/j.addr.2017.07.019

656 Lin L, Wong, H. Predicting Oral Drug Absorption: Mini Review on Physiologically-Based
657 Pharmacokinetic Models. Pharmaceutics 2017; 9 (41): 1-14.
658 https://doi.org/10.3390/pharmaceutics9040041

659 Michaelsen MH, Siqueira Jørgensen SD, Abdi IM, Wasan KM, Rades T, Müllertz A. Fenofibrate oral
660 absorption from SNEDDS and super-SNEDDS is not significantly affected by lipase inhibition in rats.
661 Eur. J. Pharm. Biopharm. 2019; 142: 258-264. https://doi.org/10.1016/j.ejpb.2019.07.002

662 Miyazaki K, Kishimoto H, Muratani M, Kobayashi H, Shirasaka Y, Inoue K. Mucins are Involved in
663 the Intestinal Permeation of Lipophilic Drugs in the Proximal Region of Rat Small Intestine. Pharm.
664 Res. 2019; 36 (162): 1-11. https://doi.org/10.1007/s11095-019-2701-9

665 Mosgaard MD, Sassene P, Mu H, Rades T, Müllertz A. Development of a high-throughput in vitro
666 intestinal lipolysis model for rapid screening of lipid-based drug delivery systems. Eur. J. Pharm.
667 Biopharm. 2015; 94: 493-500. https://doi.org/10.1016/j.ejpb.2015.06.028

668 Mosgaard MD, Sassene PJ, Mu H, Rades T, Müllertz A. High-Throughput Lipolysis in 96-Well Plates
669 for Rapid Screening of Lipid-Based Drug Delivery Systems. J. Pharm. Sci. 2017; 106:1183-1186.
670 https://doi.org/10.1016/j.xphs.2016.12.026

671 O'Dwyer PJ, Box KJ, Koehl NJ, Bennett-Lenane H, Reppas C, Holm R, Kuentz M, Griffin BT. Novel
672 Biphasic Lipolysis Method To Predict in Vivo Performance of Lipid-Based Formulations. Mol.Pharm.
673 2020; 17: 3342-3352. https://doi.org/10.1021/acs.molpharmaceut.0c00427

674 Porter CJH, Trevaskis NL, Charman WN. Lipids and lipid-based formulations: optimizing the oral
675 delivery of lipophilic drugs. Nat. Rev. Drug Discov. 2007; 6 (3): 231–248.
676 https://doi.org/10.1038/nrd2197

677 Savla R, Browne J, Plassat V, Wasan KM, Wasan EK. Review and analysis of FDA approved drugs
678 using lipid-based formulations. Drug Develop. Ind. Pharm. 2017; 43: 1743-1758.
679 https://doi.org/10.1080/03639045.2017.1342654

680 Schen JS, Burgess DJ. In Vitro-In Vivo Correlation for Complex Non-Oral Drug Products: Where Do
681 We Stand? J. Control. Release 2015; 219: 644-651. https://doi.org/10.1016/j.jconrel.2015.09.052

682 Siqueira SDVS, Müllertz A, Gräeser K, Kasten G, Mu H, Rades T. Influence of drug load and physical
683 form of cinnarizine in new SNEDDS dosing regimens: in vivo and in vitro evaluations. AAPS J. 2017;19
684 (2): 587-594. https://doi.org/10.1208/s12248-016-0038-4

685 Stillhart C, Imanidis G, Griffin BT, Kuentz M. Biopharmaceutical Modeling of Drug Supersaturation

During Lipid-Based Formulation Digestion Considering an Absorption Sink. Pharm. Res. 2014; 31:3426-3444. https://doi.org/10.1007/s11095-014-1432-1

Tanaka Y, Tay E, Nguyen TH, Porter CJH. Quantifying in vivo luminal drug solubilization-supersaturation-precipitation profiles to explain the performance of lipid based formulations. Pharm. Res. 2020; 37 (47): 1-17. https://doi.org/10.1007/s11095-020-2762-9

Thomas N, Richter K, Pedersen TB, Holm R, Müllertz A, Rades T. In vitro lipolysis data does not adequately predict the in vivo performance of lipid-based drug delivery systems containing fenofibrate. AAPS J. 2014; 16 (3): 539-549. https://doi.org/10.1208/s12248-014-9589-4

Trevaskis NL, Charman WN, Porter CJH. Lipid-based delivery systems and intestinal lymphatic drug transport: a mechanistic update. Adv. Drug Deliv. Rev. 2008; 60 (6): 702–716. https://doi.org/10.1016/j.addr.2007.09.007

Vertzoni M, Augustijns P, Grimm M, Koziolek M, Lemmens G, Parrott N, Pentafragka C, Reppas C, Rubbens J, Van Den Abeele J, Vanuytsel T, Weitschies W, Wilson CG. Impact of regional differences along the gastrointestinal tract of healthy adults on oral drug absorption: An UNGAP review. Eur. J. Pharm. Sci. 2019; 134: 153-175. https://doi.org/10.1016/j.ejps.2019.04.013

Yeap YY, Lock J, Lerkvikarn S, Semin T, Nguyen N, Carrier RL. Intestinal mucus is capable of stabilizing supersaturation of poorly water-soluble drugs. J. Control. Release 2019; 296: 107-113. https://doi.org/10.1016/j.jconrel.2018.11.023

Yeap YY, Trevaskis N, Porter CJH. Lipid absorption triggers drug supersaturation at the intestinal unstirred water layer and promotes drug absorption from mixed micelles. Pharm. Res. 2013; 30: 3045-3058. https://doi.org/10.1007/s11095-013-1104-6

Zangenberg NH, Müllertz A, Kristensen HG, Hovgaard L. A dynamic in vitro lipolysis model I. Controlling the rate of lipolysis by continuous addition of calcium. Eur. J. Pharm. Sci. 2001; 14: 115-122. https://doi.org/10.1016/s0928-0987(01)00169-5